agriculture

MDPI

Article

Sensitivity of Four Indices of Meteorological Drought for Rainfed Maize Yield Prediction in the State of Sinaloa, Mexico

Llanes-Cárdenas Omar [1,*], Norzagaray-Campos Mariano [1], Gaxiola Alberto [2], Pérez-González Ernestina [1], Montiel-Montoya Jorge [1] and Troyo-Diéguez Enrique [3]

[1] Centro Interdisciplinario de Investigación para el Desarrollo Integral Regional, Instituto Politécnico Nacional, (CIIDIR-IPN), Unidad Sinaloa, Jiquilpan 59510, Mexico; mnorzagarayc@ipn.mx (N.-C.M.); eperezg@ipn.mx (P.-G.E.); jmontielm@ipn.mx (M.-M.J.)

[2] Facultad de Ingeniería Mochis (UAS-FIM), Universidad Autónoma de Sinaloa, Fuente de Poseidón y Ángel Flores s/n, Los Mochis 81223, Mexico; alberto.gaxiola@uas.edu.mx

[3] Centro de Investigaciones Biológicas del Noroeste (CIBNOR-La Paz), Av. Instituto Politécnico Nacional 195, Playa Palo de Santa Rita Sur, La Paz 23096, Mexico; etroyo04@cibnor.mx

* Correspondence: ollanesc@ipn.mx; Tel.: +16-87-872-9625; Fax: +52-68-7872-9625

Abstract: In the state of Sinaloa, rainfall presents considerable irregularities, and the climate is mainly semiarid, which highlights the importance of studying the sensitivity of various indices of meteorological drought. The goal is to evaluate the sensitivity of four indices of meteorological drought from five weather stations in Sinaloa for the prediction of rainfed maize yield. Using DrinC software and data from the period 1982–2013, the following were calculated: the standardized precipitation index (*SPI*), agricultural standardized precipitation index (*aSPI*), reconnaissance drought index (*RDI*) and effective reconnaissance drought index (*eRDI*). The observed rainfed maize yield (RMY_{ob}) was obtained online, through free access from the database of the Agrifood and Fisheries Information Service of the government of Mexico. Sensitivities between the drought indices and RMY_{ob} were estimated using Pearson and Spearman correlations. Predictive models of rainfed maize yield (RMY_{pr}) were calculated using multiple linear and nonlinear regressions. In the models, *aSPI* and *eRDI* with reference periods and time steps of one month (January), two months (December–January) and three months (November–January), were the most sensitive. The correlation coefficients between RMY_{ob} and RMY_{pr} ranged from 0.423 to 0.706, all being significantly different from zero. This study provides new models for the early calculation of RMY_{pr}. Through appropriate planning of the planting–harvesting cycle of dryland maize, substantial socioeconomic damage can be avoided in one of the most important agricultural regions of Mexico.

Keywords: multiple linear regression; multiple nonlinear regression; socioeconomic damage

Citation: Omar, L.-C.; Mariano, N.-C.; Alberto, G.; Ernestina, P.-G.; Jorge, M.-M.; Enrique, T.-D. Sensitivity of Four Indices of Meteorological Drought for Rainfed Maize Yield Prediction in the State of Sinaloa, Mexico. *Agriculture* **2022**, *12*, 525. https://doi.org/10.3390/agriculture12040525

Academic Editor: Alexander Gröngröft

Received: 1 March 2022
Accepted: 3 April 2022
Published: 8 April 2022

1. Introduction

One of the natural phenomena that causes the most socio-environmental damage worldwide is meteorological drought (*MD*) [1]. This drought results mainly from irregular precipitation (*P*) [2,3] and high potential evapotranspiration (PET) [4].

These two climate variables can reduce the yield of rainfed agricultural crops in any region of the world [3], causing damage to crops and serious economic losses [5,6]. Mexico is no exception [5], due in part to the fact that although the state of Sinaloa is considered "the breadbasket of Mexico," it has also recently registered a substantial irregularity in *P*. This irregularity inevitably makes the socioeconomic condition vulnerable [7,8] due to low agricultural yields [9], and according to [10], especially the observed rainfed maize yield (RMY_{ob}). The rainfed corn crop in Sinaloa is particularly important because the area planted with this crop currently exceeds the area planted with irrigated corn. In addition, corn is in first place among the eight basic crops of the state [9], and the crop is the most seriously affected by irregular *P* and high temperatures [11,12].

Usually, these low RMY_{ob} are associated with only a single index of *MD*; that is, most research does not choose the most sensitive drought index, which calls into question whether the yield prediction (RMY_{pr}) is satisfactory [12–14].

Although most predictions are made with linear approximations, it is important to consider that many phenomena in nature do not behave linearly [15]. Due to this [16], recommends that more research worldwide should employ nonlinear tools, such as multiple nonlinear regression (*MNR*), which according to [17,18] in many cases yields more accurate predictions than multiple linear regression (*MLR*).

To establish suitable models of RMY_{pr} for Sinaloa, it is vital to assess sensitivity by calculating correlations between RMY_{ob} and various *MD* indices with different reference periods and early time steps [11,19,20].

Worldwide, four of the most widely used indices of *MD* are (1) standardized precipitation index (*SPI*), formulated by [21], which is based only on total *P* as input data. The authors of [22] therefore tried to increase the sensitivity [23] of the *SPI* by designing the (2) agricultural standardized precipitation index (*aSPI*), which considers only the *P* used by crops [24]. (3) The reconnaissance drought index (*RDI*), created by [25] and applied by [26], and (4) the effective reconnaissance drought index (*eRDI*), formulated by [27] and applied by [28], try to express severe drought phenomena not only with knowledge of *P* but also of potential *PET*.

The importance of the use of these four *MD* indices lies mainly in their widespread use around the world due to their simple structure, ease of use and efficiency of the results [22,29,30]. For example, [29] successfully applied the *SPI* in the semi-arid region of the Merguellil Basin in central Tunisia, managing to spatially and temporally map the extreme drought for the period 1983–2018. In the case of the *aSPI* index, [22] applied it successfully in four semi-arid areas (north-east, north, center and south) of Greece, finding that this index is more robust than the *SPI*, mainly in the identification of agricultural droughts. The four indices (*SPI*, *aSPI*, *RDI* and *eRDI*) were used jointly by [30], who applied them in Saudi Arabia (a region with a semi-arid–arid climate), for the period 1985–2020, and found a robust relationship between meteorological droughts and the Pacific decadal oscillation, which indicates a property of predictability of these dry phenomena.

In this study, for five municipalities and for the period 1982–2013, RMY_{ob} was obtained online from the database of the Agrifood and Fisheries Information Service of the government of Mexico (SIAP). Using DrinC software and information from five meteorological stations, four indices of *MD* were calculated: *SPI*, *aSPI*, *RDI* and *eRDI*. To propose models sensitive to *MD* in Sinaloa, Pearson and Spearman correlations were applied between the four indices of *MD* and RMY_{ob}. To obtain the RMY_{pr}, *MLR* and *MNR* were applied between the indices of *MD* (with the highest significant correlation) and RMY_{ob}. To find out if the RMY_{pr} values were significantly different from zero, Pearson and Spearman correlations and a hypothesis test were applied between RMY_{ob} and RMY_{pr}.

The goal was to evaluate the sensitivity of the four indices of MD for the calculation of RMY_{pr} from five meteorological stations in Sinaloa.

This study provides new models (based on four indices of *MD* widely used around the world) for the early calculation of RMY_{pr}, which can help avert environmental damage and considerable socioeconomic losses [31] in one of the Mexican states that produces the most rainfed maize [9,32].

2. Materials and Methods

2.1. Study Area

The study area was located in northwestern Mexico (Figure 1), specifically in the central-southern part of the state of Sinaloa. Data from five meteorological stations in this region were used; Culiacán, La Concha, Las Tortugas, Rosario and Sta. Cruz de A., located in the municipalities of Culiacán, Escuinapa, Concordia, Rosario and Cosalá, respectively. The state of Sinaloa has a high volume of agricultural activity, so much so that it is often called "the breadbasket of Mexico" [33]. The largest proportion of Sinaloa has a climate ranging in a

north–south direction from arid to semi-arid, and in some southern municipalities, a climate that becomes warm sub-humid [34]. Approximately 70% of the total annual *P* falls in the summer (June–September) [35]. For the study area, the following are the annual values for the period 1982–2013 of the average (*avg.*), standard deviation (*SD*), variance (*Va*) and coefficient of variation (*C.V.*) for *P* (*avg.* = 860.96 mm, *SD* = 132.49 mm, *Va* = 17552.36 mm^2 and *C.V.* = 15%), *Tmax* (*avg.* = 32.98 mm, *SD* = 0.40 mm, *Va* = 0.16 mm^2 and *C.V.* = 1%), *Tmin* (*avg.* = 17.97 mm, *SD* = 0.97 mm, *Va* = 0.94 mm^2 and *C.V.* = 5%), *PET* (*avg.* = 1881.61 mm, *SD* = 59.70 mm, *Va* = 3563.85 mm^2 and *C.V.* = 3%) and *A.I.* (*avg.* = 0.46, *SD* = 0.08, *Va* = 0.01 and *C.V.* = 17%).

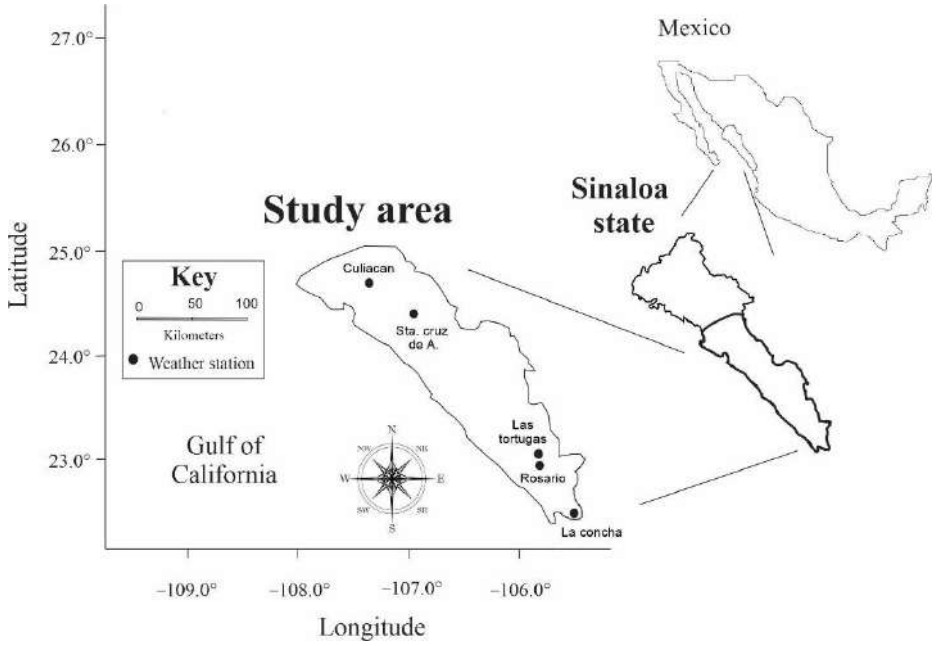

Figure 1. Study area, located in northwestern Mexico.

2.2. Data

2.2.1. Precipitation (*P*), Maximum Temperature (*Tmax*) and Minimum Temperature (*Tmin*)

Data from 70 weather stations in the state of Sinaloa were downloaded from the CLImate COMputing (CLICOM) database [36] (http://clicomex.cicese.mx, accessed on 31 December 2021) and analyzed. These weather stations were selected for the following characteristics: (1) daily availability of the data series (*P*, *Tmax* and *Tmin*) >95% [37], (2) data ≥30 years [20] and (3) annual data of RMY_{ob} = 100%. The missing *P*, *Tmax* and *Tmin* data were estimated by means of a simple imputation method (nearest neighbor), as [38,39] note that when the percentage of missing data < 5, any imputation method works well. After data quality analysis, it was decided that the study period would be 1982–2013. *P*, *Tmax* and *Tmin* data were ordered from October to September, because this is the format accepted by the DrinC software.

2.2.2. Observed Rainfed Corn Yield (RMY_{ob})

The RMY_{ob} values were obtained from the database of the Agrifood and Fisheries Information Service of the government of Mexico, at the website [40] http://infosiap.siap.gob.mx/aagricola_siap_gb/ientidad/index.jsp, accessed on 3 January 2022. In this database, only for the period 1982–2002 was the variation not recorded by municipality, so in this study, and only for this period (1982–2002), the variation of RMY_{ob} was the same for the five municipalities. Sowing and harvesting of rainfed maize in Sinaloa are usually carried out up to 31 July and 31 January, respectively [9,32].

2.3. Mathematical Expressions on Which the Indices of Meteorological Drought (MD) Are Based

2.3.1. Standardized Precipitation Index (*SPI*)

For the *SPI* index, only *P* is required as input for various time scales (1–24 months). In this index, the series are fit to the gamma probability distribution (shown in Equation (1)), to then convert this distribution to the standard normal probability distribution [21]; that is, the average *SPI* will have a null value [14].

$$g(x) = \frac{1}{\beta^{\alpha}\Gamma(\alpha)} x^{\alpha-1} e^{\frac{-x}{\beta}}, \text{for } x > 0 \quad (1)$$

where α and β are the shape and scale parameters, respectively (calculated for each weather station and time scale in months). $\Gamma(\alpha)$ is the gamma function and x is *P*. The maximum likelihood functions for α and β are given by Equations (2) and (3):

$$\alpha = \frac{1}{4A}\left(1 + \sqrt{1 + \frac{4A}{3}}\right) \quad (2)$$

$$\beta = \frac{\bar{x}}{\alpha}, \quad (3)$$

$$\text{where } A = ln\left(\bar{x}\right) - \frac{\sum ln(x)}{n} \quad (4)$$

In Equation (4), n is the number of observations. As $\Gamma(\alpha)$ is not defined for $x = 0$ and since the values of a series of *P* can be zero, the probability is the expression given in Equation (5):

$$H(x) = q + (1-q)\cdot G(x) \quad (5)$$

where q is the probability of the absence of *P* and *G(x)* is the incomplete cumulative probability of $\Gamma(\alpha)$. If m is the number of nulls in a series of *P*, then q can be estimated as m/n. *H(x)* is the standard normal random variable z, with *avg.* = zero and *Va* = 1 [14].

2.3.2. Agricultural Standardized Precipitation Index (*aSPI*)

For the *aSPI*, the cumulative probability distribution is transformed into a normal distribution through the approximation of Equation (6) [21,22]:

$$aSPI = -\left(t - \frac{c_0 + c_1 t + c_2 t^2}{1 + d_1 t + d_2 t^2 + d_3 t^3}\right), \ 0 < H(x) \leq 0.5 \quad (6)$$

$$\text{where } t = \sqrt{ln\frac{1}{H(x)^2}} \quad (7)$$

$$aSPI = t - \frac{c_0 + c_1 t + c_2 t^2}{1 + d_1 t + d_2 t^2 + d_3 t^3}, \ 0.5 < H(x) \leq 1.0 \quad (8)$$

$$\text{where } t = \sqrt{ln\frac{1}{[1-H(x)^2]}} \quad (9)$$

$$\text{and } c_0 = 2.515517, c_1 = 0.802853, \ \ c_2 = 0.010328, d_1 = 1.43278, d_2 = 0.189269, \ d_3 = 0.001308$$

2.3.3. Reconnaissance Drought Index (*RDI*)

The *RDI* index can be calculated using three expressions, the first being the initial value of *RDI*, shown in Equation (10):

$$\alpha_0^{(i)} = \frac{\sum_{j=1}^{12} P_{ij}}{\sum_{j=1}^{12} PET_{ij}}, \ i = 1(1)\cdot N, \ \text{where } \ j = 1(1)\cdot 12 \quad (10)$$

where P_{ij} and PET_{ij} are P and PET of the jth month of the ith year and N is the number of years of data available [14].

The second expression yields the normalized *RDI*, using Equation (11):

$$\boldsymbol{RDI_n^{(i)}} = \frac{\boldsymbol{\alpha_0^{(i)}}}{\boldsymbol{\overline{\alpha}_0}} - 1, \tag{11}$$

where $\overline{\alpha}_0$ is the *avg.* of α_0 and N is the number of years.

The third expression, giving the standardized *RDI*, is shown in Equation (12):

$$\boldsymbol{RDI_{st(k)}^{(i)}} = \frac{\boldsymbol{y_k^{(i)}} - \boldsymbol{\overline{y}_k}}{\boldsymbol{\hat{\sigma}_{yk}}} \tag{12}$$

where y_i is ln $\alpha_0^{(i)}$, $\overline{y}_k$ is the *avg.* and $\hat{\sigma}_{yk}$ is the *SD*. The standardized *RDI* expression is based on the assumption that α_0 follows a log-normal distribution [14].

2.3.4. Effective Reconnaissance Drought Index (*eRDI*)

The *eRDI* is calculated from P and PET (Equation (13)), where α is the initial form of the index for one year and for a reference period of k months, as shown in Equation (13):

$$\boldsymbol{\alpha_k} = \frac{\sum_{j=1}^{j=k} \boldsymbol{P_j}}{\sum_{j=1}^{j=k} \boldsymbol{PET_j}} \tag{13}$$

where P_j is modified by P_{ej}, which refers to the effective monthly P in month j, and α_k is modified by α_{ek}, which is the initial form of the effective index; see Equation (14):

$$\boldsymbol{\alpha_{e(k)}} = \frac{\sum_{j=1}^{j=k} \boldsymbol{P_{ej}}}{\sum_{j=1}^{j=k} \boldsymbol{PET_j}} \tag{14}$$

Effective P is always based on monthly total P values and not on values for the entire reference period [28].

The *eRDI* indexes in the normalized and standardized forms are calculated with procedures similar to those for the *RDI* index.

2.4. Determination of Each of the Indices of Meteorological Drought (MD)

Using DrinC software, the *SPI*, *aSPI*, *RDI* and *eRDI* indices were calculated for the early reference periods [11] and time frames of 1 month (January), 2 months (December–January), 3 months (November–January) and 6 months (October–January). Prior to obtaining the four MD indices, the program was fed with monthly data of P, *Tmax* and *Tmin*, previously calculated through daily data series. Two intermediate calculations were (1) *PET*, by the Hargreaves method [41] and (2) the aridity index (*AI*), by the UNEP method [42–44]. To obtain *aSPI* and *eRDI*, the effective P was calculated using the USDA method (CROPWAT version), as it is a widely used method for arid and semi-arid climates [22,45]. Table 1 shows a classification of the four indices of *MD* in Sinaloa based on the classification proposed by [24,46]. This classification is similar to the one proposed by [30].

Table 1. Classification of the indices *SPI*, *aSPI*, *RDI* and *eRDI* for Sinaloa. Source: Authors, from (Tsakiris et al. (2007) and Proutsos and Tigkas (2020) [26,46]).

***SPI*, *aSPI*, *RDI* and *eRDI* (Dimensionless)**	**Category**
≥2.00	Extremely wet
1.5 to 1.99	Severely wet
1.0 to 1.49	Moderately wet
0.0 to 0.99	Mildly wet
0.0 to −0.99	Mild drought
−1.00 to −1.49	Moderate drought
−1.50 to −1.99	Severe drought
≤−2.00	Extreme drought

2.5. Z Normalization

To remove the measurement units [32], and to be able to apply the correlation and regression analyses to the *SPI*, *aSPI*, *RDI* and *eRDI* indices and RMY_{ob}, a standardized Z normalization was applied. This normalization method consists of subtracting the average from each value of each series and dividing the result by the standard deviation [47]. This process was applied to annual data from the five meteorological stations (*P*, *Tmax* and *Tmin*) for the period 1982–2013.

2.6. Statistical Analysis

2.6.1. Normality, Correlation and Hypothesis Test between the *SPI*, *aSPI*, *RDI*, *eRDI* Indices and Observed Rainfed Maize Yield (RMY_{ob})

To establish whether a Pearson ($r'P$) or Spearman ($r'S$) correlation would apply, a Shapiro–Wilk normality analysis was performed on all standardized time series [48]. An $r'P$ was applied to the series that did present normality, and $r'S$ was applied to the series that did not present normality. To identify whether $r'P$ and $r'S$ were significantly $\neq 0$, a hypothesis test was applied (*H0:* $r'P$ *and* $r'S \neq 0$*; H1:* $r'P$ and $r'S = 0$). This test contrasted the coefficients $r'P$ and $r'S$ with the critical correlation coefficients of Pearson ($r'P_{cr} = |0.339|$; $n = 32$) and Spearman ($r'S_{cr} = |0.338|$; $n = 32$), which were obtained from [49].

2.6.2. Models for Predicted Rainfed Maize Yield (RMY_{pr})

To obtain RMY_{pr}, *MLR* [10,50] were initially applied, with the best model variable selection method. For the models that did not present normality in the residuals, an *MNR* was applied. The *MNR* was employed because this predictive model presented the highest coefficient of determination (R^2). In addition, [18] point out that it is a more efficient predictive tool than *MLR*. In order to choose the best model (highest R^2), combinations of variables that presented the highest correlations from each weather station were used (Table 2).

Table 2. Average, maximum and minimum values of *P*, *Tmax*, *Tmin* and *PET*, and average value of *A.I.*

		Weather Station				
Climate Indicator	**Statistical Inference**	**Culiacan**	**La Concha**	**Las Tortugas**	**Rosario**	**Sta. Cruz de A.**
P (mm year^{-1})	Average	681.85	1027.97	913.59	898.34	783.06
	Max	1180.70	1623.10	1606.30	1337.30	1254.58
	Min	445.95	584.56	536.40	607.04	354.88
Tmax (°C year^{-1})	Average	33.28	32.73	33.44	32.45	32.97
	Max	35.30	35.18	35.26	33.41	34.48
	Min	31.63	26.44	31.11	30.54	31.83
Tmin (°C year^{-1})	Average	18.36	18.76	16.51	18.74	17.45
	Max	21.10	20.82	18.54	19.81	18.97
	Min	16.30	15.29	14.77	17.45	15.21
PET (mm year^{-1})	Average	1890.59	1845.52	1965.37	1807.18	1899.39
	Max	2066.29	1987.68	2075.08	1891.61	2067.52
	Min	1789.37	1435.05	1757.29	1595.92	1770.32
A.I. (dimensionless)	Average	0.36	0.56	0.46	0.50	0.41

2.6.3. Validation of the Prediction Models: Normality, Correlation and Hypothesis Testing for Observed Rainfed Maize Yield (RMY_{ob}) and Predicted Rainfed Maize Yield (RMY_{pr})

An *r'P* (data series with normality) and an *r'S* (data series without normality) were applied between RMY_{ob} and RMY_{pr}. To determine whether the correlations were significantly different from zero, a hypothesis test was performed. In this section, the tests of normality and hypotheses also used Shapiro–Wilk and contrasted the critical correlation coefficients of Pearson and Spearman, as previously indicated. In this study, all statistical analyses were evaluated with a significance level of $\alpha = 0.05$.

The programs used were Microsoft Excel 365, XLstat version 2021, PAleontological STatistics (PAST) version 4.08, and CorelDRAW version 2019.

3. Results

3.1. Aridity Index (A.I.)

The lowest *P*, 354.88 mm year^{-1}, was recorded at Sta. Cruz de A.; the highest *Tmax* and highest *Tmin*, 35.30 °C year^{-1} and 21.10 °C year^{-1}, respectively, were recorded at Culiacán; and the highest *PET* was 2075.08 mm year^{-1}, recorded at Las Tortugas (Table 2). Only the La Concha station presented dry sub-humid conditions (A.I. = 0.56), the remaining four stations being classified as semi-arid (A.I. $\leq$ 0.50).

3.2. Statistical Analysis

Normality, Correlation and Hypothesis Test between the *SPI*, *aSPI*, *RDI*, *eRDI* Indices and Observed Rainfed Maize Yield (RMY_{ob}).

The only pair of data series that did present normality were aSPI-3 (p-value = 0.300) and RMY_{ob} (p-value = 0.103), for the Culiacán station. The p-values for the remaining four stations are: La Concha, *aSPI-3* (p-value = 0.071) vs. RMY_{ob} (p-value = 0.030); Las Tortugas, *aSPI-3* (p-value = 0.041) vs. RMY_{ob} (p-value = 0.661); Rosario, *aSPI-3* (p-value = 0.016) vs. RMY_{ob} (p-value = 0.006) and Sta. Cruz de A., *aSPI-3* (p-value = 0.083) vs. RMY_{ob} (p-value = 0.001).

The index that registered the greatest sensitivity to *MD* is *aSPI-3* (November–January). Although the five weather stations presented a significant correlation (Culiacan, *r'P* = −0.347; La Concha, *r'S* = −0.427; Las Tortugas, *r'S* = −0.475; Rosario, *r'S* = −0.468 and Rosario, *r'S* = −0.381), four presented 0.50 $\geq$ *A.I.* $\geq$ 0.20 (semi-arid climate). El Rosario and Sta. Cruz de A. stations recorded the highest number of significant correlations, eight in each case; however, the highest magnitudes were recorded at El Rosario; *SPI-3* (November–January) = −0.460; *aSPI-3* (November–January) = −0.468, *RDI-3* (November–January) = −0.448 and *eRDI-3*

(November–January) = −0.461 (Table 3). Because the 3-month reference period (November–January) had the highest number of significant correlations for the four indices of *MD* (Table 3), in Figures 2a–e and 3a–e, it was decided to show the variations of *SPI-3*, *aSPI-3*, *RDI-3* and *eRDI-3* for the time frame (November–January).

Table 3. Coefficients of *r'P* and *r'S*, between the *SPI*, *aSPI*, *RDI* and *eRDI* indices, and RMY_{ob}.

Drought Index with Reference Period and Time Frame	Weather Station				
	Culiacán	**La Concha**	**Las Tortugas**	**Rosario**	**Sta. Cruz de A.**
SPI-1 (January)	−0.124	−0.304	−0.301	**−0.348**	**−0.397**
SPI-2 (December–January)	−0.103	−0.322	−0.248	−0.309	−0.328
SPI-3 (November–January)	**−0.344**	**−0.421**	**−0.453**	**−0.460**	**−0.387**
SPI-6 (August–January)	−0.268	0.110	0.128	0.141	−0.201
aSPI-1 (January)	−0.124	−0.304	−0.301	**−0.348**	**−0.397**
aSPI-2 (December–January)	−0.112	−0.324	−0.253	−0.314	−0.333
aSPI-3 (November–January	**−0.347**	**−0.427**	**−0.475**	**−0.468**	**−0.381**
aSPI-6 (August–January)	−0.229	−0.238	−0.021	−0.199	−0.281
RDI-1 (January)	−0.134	−0.288	−0.305	**−0.348**	**−0.395**
RDI-2 (December–January)	−0.103	−0.323	−0.270	−0.319	−0.329
RDI-3 (November–January)	−0.311	**−0.381**	**−0.480**	**−0.448**	**−0.385**
RDI-6 (August–January)	−0.257	0.148	0.097	0.147	−0.273
eRDI−1 (January)	−0.134	−0.288	−0.305	**−0.348**	**−0.395**
eRDI-2 (December–January)	−0.112	−0.321	−0.270	−0.319	−0.331
eRDI-3 (November–January)	−0.312	**−0.408**	**−0.474**	**−0.461**	**−0.376**
eRDI-6 (August–January)	−0.221	−0.191	−0.049	−0.166	−0.292
$r'S_{cr}$ = |0.338|; *n* = 32	Bold = significant correlation				
$r'P_{cr}$ = |0.339|; *n* = 32					

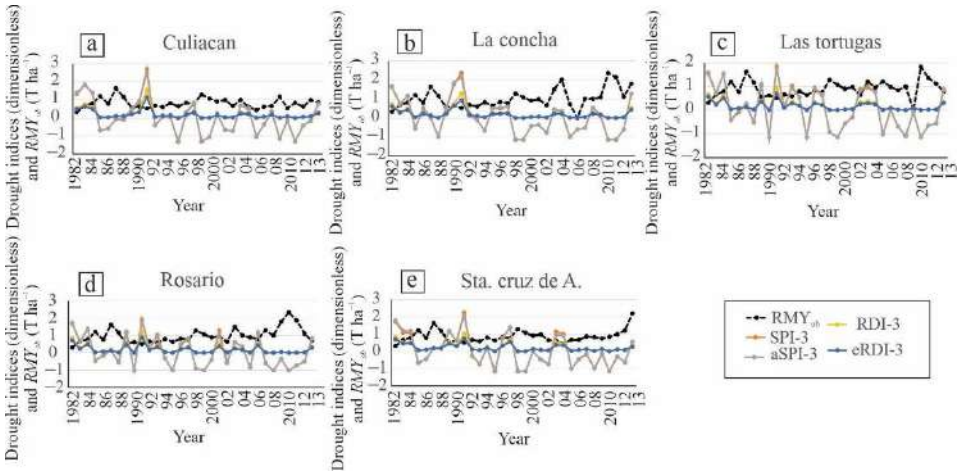

Figure 2. Annual variation (dimensionless) of the *SPI-3*, *aSPI-3*, *RDI-3* and *eRDI-3*, and RMS_{ob} indices (T ha^{-1}). The black line refers to RMY_{ob} and the four meteorological drought indices in Sinaloa are shown in red (*SPI-3*), gray (*aSPI-3*), yellow (*RDI-3*) and blue (*eRDI-3*) (**a**–**e**).

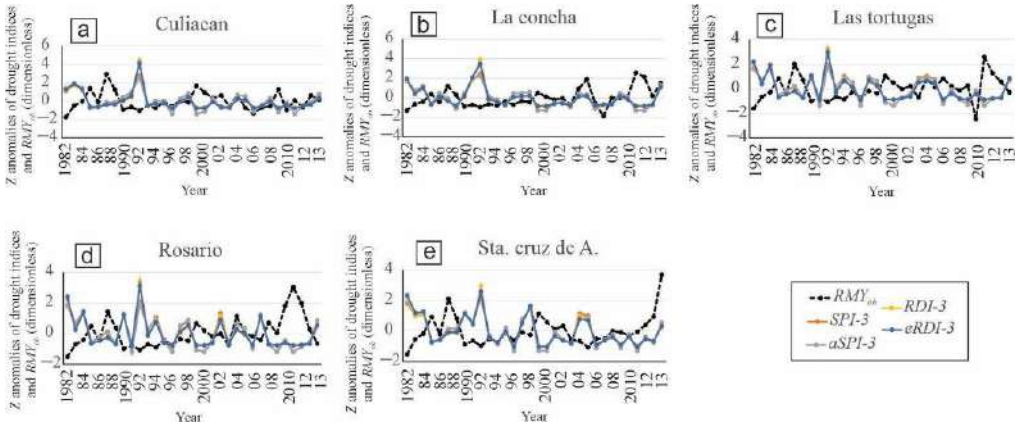

Figure 3. *Z* anomalies of the drought indices *SPI-3*, *aSPI-3*, *RDI-3* and *eRDI-3*, and RMY_{ob} (dimensionless). The black line refers to RMY_{ob} and the four meteorological drought indices in Sinaloa are shown in red (*SPI-3*), gray (*aSPI-3*), yellow (*RDI-3*) and blue (*eRDI-3*) (**a**–**e**).

3.3. Variation of SPI-3, aSPI-3, RDI-3 and eRDI-3 Indices, and RMY_{ob}

SPI-3 and *aSPI-3* indices for the five stations (Figure 2a–e) registered very similar magnitudes; however, for Culiacán (Figure 2a), coincidentally both the highest (in 1991) and lowest (in 1995) magnitudes were registered. These values were for *SPI-3* (from −1.32 to 2.68) and for *aSPI* (from −1.32 to 2.48) respectively, and are classified from moderately dry to extremely humid *MD* values (Table 1).

3.4. Z Normalization

The highest magnitudes were recorded for 1991 at the Culiacán station (*eRDI-3* = 4.11; Figure 3a) and La Concha station (*RDI-3* = 3.91; Figure 3b). The minimum values were recorded at the Culiacán station (*aSPI-3* = −1.42 and *SPI-3* = −1.40; Figure 3a) for 1998. The minimum value of yield was recorded for Las Tortugas in 2009 (RMY_{ob} = −2.46; Figure 3c).

3.5. Models for Calculating Predicted Rainfed Maize Yield (RMY_{pr}): Normality, Correlation and Hypothesis Test

From the results of the initial *MLR*, only the Culiacán station (Figure 4a) presented normality in the residuals (*p*-value = 0.68), with $r'P = 0.502$ and $R^2 = 0.252$. The $r'S$ and R^2 for the four remaining weather stations (Figure 4b–e) are La Concha ($r'S = 0.423$; $R^2 = 0.179$), Las Tortugas ($r'S = 0.569$; $R^2 = 0.324$), Rosario ($r'S = 0.706$; $R^2 = 0.499$) and Sta. Cruz de A. ($r'S = 0.6259$; $R^2 = 0.392$).

The 32-year variations of RMY_{ob} and RMY_{pr} for the five meteorological stations are shown in Figure 5a–e, as well as the five equations of the respective models.

$$Culiacan = 0.83 + 0.23(aSPI - 2) - 0.22(aSPI - 3) - 0.06(SPI - 6) - 0.06(aSPI - 2)(aSPI - 3) \quad (15)$$

$$La\ Concha = 1.02 + 0.23(aSPI - 1) - 0.05(aSPI - 2) - 0.06(aSPI - 3) - 0.12(aSPI - 6) - 0.37(aSPI - 1)^2 + 0.28(aSPI - 2)^2 + 0.03(aSPI - 3)^2 - 0.12(aSPI - 6)^2 \quad (16)$$

$$Las\ Tortugas = 1.09 - 0.61(eRDI - 1) + 0.09(eRDI - 2) - 0.69(RDI - 3) + 0.04(SPI - 6) + 0.84(eRDI - 1)^2 + 0.61(eRDI - 2)^2 - 0.95(RDI - 3)^2 - 0.05(SPI - 6)^2 \quad (17)$$

$$Rosario = 1.43 - 1.37(aSPI - 1) + 0.61(eRDI - 2) - 0.26(aSPI - 3) - 0.09(aSPI - 6) + 0.89(aSPI - 1)^2 - 1.03(eRDI - 2)^2 - 0.15(aSPI - 3)^2 - 0.06(aSPI - 6)^2 \quad (18)$$

$$Sta.\ Cruz\ de\ A. = -0.19 - 0.40(aSPI - 1) + 0.11(aSPI - 2) + 0.02(SPI - 3) + 6.44(eRDI - 6) + 0.11(aSPI - 1)^2 + 0.03(aSPI - 2)^2 - 0.19(SPI - 3)^2 - 7.75(eRDI - 6)^2 \quad (19)$$

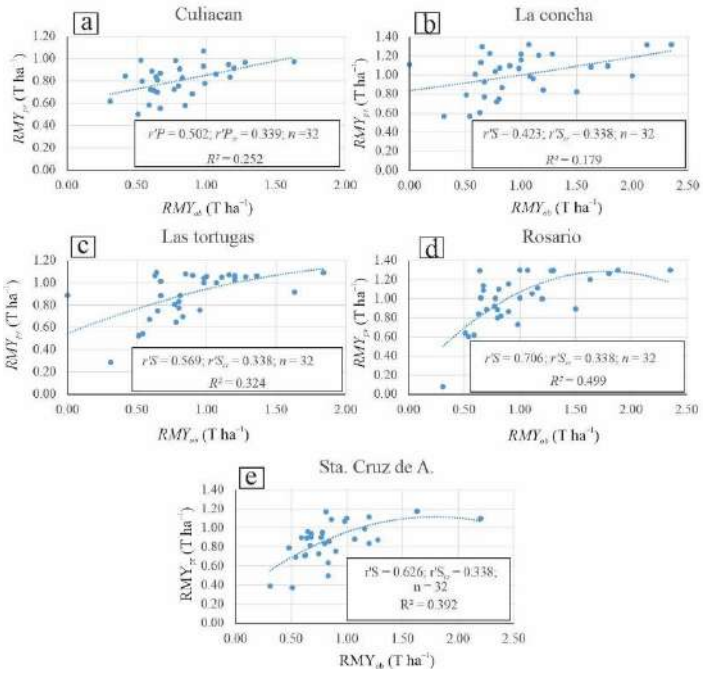

Figure 4. Validation of the models for RMY_{pr} (T ha^{-1}). (**a**) shows the single model with MLR and (**b**–**e**) show the four models with MNR.

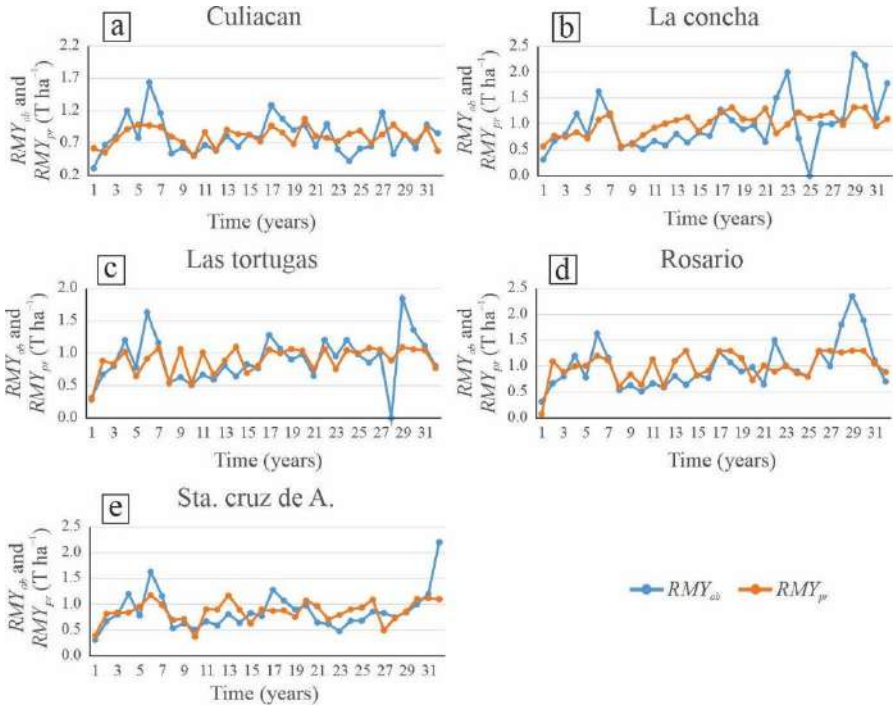

Figure 5. Annual variation of RMY_{ob} and RMY_{pr} (T ha^{-1}) (**a**–**e**). Rosario is the station with the greatest predictive capacity. The predictive capacity of the five models (Equations (15)–(19)) is low ($R^2 < 0.500$) but significantly different from zero, especially for Las Tortugas (Equation (17)), Rosario (Equation (18)) and Sta. Cruz de A. (Equation (19)) for aSPI and eRDI for one month (January), two months (December–January) and three months (November–January).

4. Discussion

The results of *A.I.* are similar to those reported by [51], who state that the climates of Sinaloa range from sub-humid temperate to very warm and dry, presenting semi-arid tropical agroclimates in the southwestern part [52].

The fact that only a couple of the series presented normality is in agreement with [15], who argues that many phenomena in nature do not behave linearly; thus, there are alternatives for data transformation, or the use of the Spearman correlation [35,53].

According to Table 3, the highest *r'P* and *r'S*, which were registered for *aSPI-3* (November–January) and *eRDI-3* (November–January), can be attributed to the fact that effective *P*, implicit in the calculation of these two indexes, is more sensitive to variations in the use of rainfed maize water [46,54], in addition to the fact that *aSPI* is an index that should be used preferentially in semi-arid climates, especially when increased sensitivity is desired [11,22,46].

The high correlation of the three-month reference period (November–January) between the *SPI*, *aSPI*, *RDI* and *eRDI* indices and RMY_{ob} is similar to that reported by [11], who argue that in the presence of *MD*, using *RDI* for reference periods of one and two months, the yield of sorghum can be successfully correlated; however, for 3-month periods, there may be a clear improvement in the early identification of drought in most cases [20].

The highest and lowest magnitudes of *aSPI* and *SPI* shown in Figure 2a agree with what was reported by [32,55], who point out that the oceanic El Niño index for 1991 registered a warm phase, which characterized an El Niño event (phase > 0.50) and for 1995, it registered a cold phase that was close to a La Niña event (phase > −0.50).

The high magnitudes of *eRDI-3* for Culiacán (Figure 3a) and *RDI* for La Concha (Figure 3b) in 1991 were associated with the occurrence of an El Niño event, which according to [56] was recorded in the period 1991–1992 and affected the Gulf of California (Sinaloa coast).

The minimum values of *SPI* and *aSPI*, recorded at the Culiacán station for 1998 (Figure 3a), were associated with the following oceanic indices anomalies: negative for the Pacific decadal oscillation, positive for the Atlantic multidecadal oscillation, negative for the oceanic El Niño index and negative for sea surface temperature in the equatorial and Caribbean seas, and positive for geopotential height in the coastal zone of Sinaloa [32,55].

The minimum value of RMY_{ob}, recorded in Las Tortugas for 2009 (Figure 3c), is attributed to the fact that in the same year, the two most extreme minimum anomalies of the period 1980–2012 were presented: (1) positive anomaly of the Pacific decadal oscillation (condition associated with the El Niño episode) and (2) negative anomaly of the Atlantic multidecadal oscillation (condition associated with the La Niña episode), which are considered to generate *P* [32,57].

The low magnitudes of RMY_{ob} (<1.0 T ha^{-1}, Figure 2) are consistent with what was found, for example, by [32,58], who argue that in the years 1990, 1997–2001, 2003, 2005 and 2008–2013, there were low magnitudes of *P* and extreme *MD*, which are associated with the occurrence of low magnitudes of sea surface temperature in the equatorial and Caribbean seas and with low magnitudes of geopotential height at the 700 hPa level on the Sinaloan coast. The minimum RMY_{ob} registered in 1982 for the Culiacán, Rosario and Sta. Cruz de A. stations were associated with the intense cyclonic *P* that occurred in the period 1982–1984 [58], which could damage maize yields by waterlogging. All these dry and wet periods mentioned by [32,58] were also recorded in this study.

The equations of models 15–17 were sensitive, which agrees with [11,22,46,54], who argue that in arid and semi-arid climates, the *MD* indices are more sensitive when effective *P* is used early.

5. Conclusions

- The sensitivity of four indices of *MD* (*SPI*, *aSPI*, *RDI* and *eRDI*) is estimated to calculate RMY_{pr}.

- The four drought indices are used with four reference periods and time steps of one month (January), two months (December–January), three months (November–January) and six months (August–January).
- The most sensitive models are for the Las Tortugas, Rosario and Sta. Cruz de A. weather stations, which include the *aSPI* and *eRDI* indices in their equations, with reference periods and time frames of one (January), two (December–January) and three months (November–January).
- In Sinaloa, it is of vital importance to calculate indices of *MD* in which effective *P* is included as the main parameter, mainly because these indices respond with greater sensitivity in arid and semi-arid conditions.
- At all five weather stations, the correlations between RMY_{ob} and RMY_{pr} are significantly different from zero.
- It is recommended to apply these predictive models to each subregion (municipality) of southern Sinaloa, in order to have reliable early predictions, especially when it is desired to prevent severe socioeconomic damage in one of the Mexican states historically the most important for the production of rainfed maize.
- In future research, it is recommended to add more predictor variables (indices of meteorological drought or environmental variables) to try to increase the predictive capacity (R^2) of the models. Some examples could be the standardized precipitation and evapotranspiration index, crop moisture index, Palmer drought severity index, minimum temperature and severe cold index.

Author Contributions: Data curation, N.-C.M., G.A. and P.-G.E.; Visualization, M.-M.J. and T.-D.E.; Writing–review & editing, L.-C.O. All authors have read and agreed to the published version of the manuscript.

Funding: Thanks are expressed for support from the Research and Postgraduate Secretariat of the National Polytechnic Institute (SIP-IPN), provided through the project with registration SIP20211457.

Institutional Review Board Statement: Not applicable.

Informed Consent Statement: Not applicable.

Data Availability Statement: http://clicom-mex.cicese.mx/mapa.html (accessed on 3 January 2022) and http://infosiap.siap.gob.mx/aagricola_siap_gb/ientidad/index.jsp (accessed on 3 January 2022).

Conflicts of Interest: The authors declare no conflict of interest.

References

1. Ochieng, P.; Nyandega, I.; Wambua, B. Spatial-temporal analysis of historical and projected drought events over Isiolo County, Kenya. *Theor. Appl. Climatol.* **2022**, *148*, 531–550. [CrossRef]
2. Bandak, S.; Movahedi, N.S.A.R.; Zeinali, E.; Bandak, I. Effects of superabsorbent polymer A200 on soil characteristics and rainfed winter wheat growth (*Triticum aestivum* L.). *Arab. J. Geosci.* **2021**, *14*, 712. [CrossRef]
3. Naveen, P.S.; Anand, B.; Srivastava, S.K.; Kumar, N.R.; Sharma, S.; Bal, S.K.; Rao, K.V.; Prabhakar, M. Risk, perception and adaptation to climate change: Evidence from arid region, India. *Nat. Hazards* **2022**, *1*, 1–24. [CrossRef]
4. He, H.; Wu, Z.; Li, D.; Zhang, T.; Pan, F.; Yuan, H.; Jiang, S.; Shi, Z.; Yang, S.; Wang, F. Characteristics of winter wheat evapotranspiration in Eastern China and comparative evaluation of applicability of different reference evapotranspiration models. *J. Soil. Sci. Plant Nutr.* **2022**. [CrossRef]
5. Núñez, L.J.M.; Cansino, L.B.; Sanchez, Z.X.G.; Ponce, O.J.M. Involving resilience in assessment of the water–energy–food nexus for arid and semiarid regions. *Clean. Techn. Environ. Policy* **2022**. [CrossRef]
6. Topçu, E.; Seçkin, N.; Açanal, H.N. Drought analyses of Eastern Mediterranean, Seyhan, Ceyhan, and Asi Basins by using aggregate drought index (ADI). *Theor. Appl. Climatol.* **2022**, *147*, 909–924. [CrossRef]
7. Martínez, S.A.R.; Villanueva, D.J.; Correa, D.A.; Estrada, Á.J.; Trucíos, C.R.; Estrada, A.J.R.; Cardoza, M.G.F.; Garza, M.M.Á. Dendroclimatic reconstruction of precipitation and temperature for the Mayo River basin in northwestern Mexico. *Trees* **2022**. [CrossRef]
8. Liu, Z.; Li, W.; Wang, L.; Li, L.; Xu, B. The scenario simulations and several problems of the Sponge City construction in semi-arid loess region, Northwest China. *Landscape Ecol. Eng.* **2022**, *18*, 95–108. [CrossRef]
9. Secretaría de Agricultura, Ganadería, Desarrollo Rural, Pesca y Alimentación (SAGARPA). *Agenda Técnica Agrícola de Sinaloa, Segunda Edición*; SAGARPA: Mexico City, Mexico, 2015; p. 242.

10. Ojeda, B.W. Evaluación del impacto del cambio climático en la productividad de la agricultura de riego y temporal del estado de Sinaloa. *Inf. Final. De Proy. De Investig.* **2010**, *45*, 393.
11. Tigkas, D.; Tsakiris, G. Early estimation of drought impacts on rainfed wheat yield in mediterranean climate. *Environ. Process.* **2015**, *2*, 97–114. [CrossRef]
12. Dos Santos, A.C.C.; Neale, M.U.C.; Mekonnen, M.M.; Goncalves, Z.I.; Oliveira, G.; Álvarez, R.O.; Safa, B.; Rowe, M.C. Trends o extreme air temperature and precipitation and their impact on corn and soybean yileds in Nebraska, USA. *Theor. Appl. Climatol.* **2022**, *147*, 1379–1399. [CrossRef]
13. Ozturk, A.; Erdem, E.; Aydin, M.; Murat, K.M. The effects of drought after anthesis on the grain quality of bread wheat depend on drought severity and drought resistance of the variety. *Cereal Res. Commun.* **2022**, *50*, 105–116. [CrossRef]
14. Tigkas, D.; Vangelis, H.; Tsakiris, G. DrinC: A software for drought analysis based on drought indices. *Earth. Sci. Inform.* **2015**, *8*, 697–709. [CrossRef]
15. Figueroa, S.C. Modelo de Regresión No Lineal. S.l. Bachelor's Thesis, Instituto Politécnico Nacional, Universidad de Buenos Aires, Buenos Aires, Argentina, 2013; 51p.
16. Zuluaga, G.O.A.; Patiño, Q.J.E.; Valencia, H.G.M. Modelos implementados en el análisis de series de tiempo de temperatura superficial e índices de vegetación: Una propuesta taxonómica en el contexto de cambio climático global. *Rev. Geog. Nor. Gran.* **2021**, *78*, 323–344. [CrossRef]
17. Fan, C.; Ding, Y. Cooling load prediction and optimal operation of HVAC systems using a multiple nonlinear regression model. *Ener. Build.* **2019**, *197*, 7–17. [CrossRef]
18. Wang, Z.; Chen, J.; Zhang, J.; Tan, X.; Ali, R.M.; Ma, J.; Zhu, Y.; Yang, F.; Yang, W. Assessing canopy nitrogen and carbon content in maize by canopy spectral reflectance and uninformative variable elimination. *Crop. J.* **2022**. [CrossRef]
19. Mekuria, G.; Legesse, A.; Mohammed, Y. Socioeconomic vulnerability of pastoralism under spatiotemporal patterns of drought in Eastern Africa. *Arab. J. Geosci.* **2021**, *14*, 2654. [CrossRef]
20. Ilyas, A.M.; Elahi, E.; Chand, R.; Zhu, D.; Muhammad, J.; Rafique, D.M.; Majid, S.A.; Ali, K.M. Estimation of a trend of meteorological and hydrological drought over Qinhuai River Basin. *Theor. Appl. Climatol.* **2022**, *147*, 1065–1078. [CrossRef]
21. McKee, T.B.; Doeskin, N.J.; Kleist, J. The relationship of drought frequency and duration to time scales. In Proceedings of the 8th Conference on Applied Climatology, Anaheim, CA, USA, 17–22 January 1993; American Meteorological Society: Boston, MA, USA, 1993; pp. 179–184.
22. Tigkas, D.; Vangelis, H.; Tsakiris, G. Drought characterisation based on an agriculture-oriented standardised precipitation index. *Theor. Appl. Climatol.* **2019**, *135*, 1435–1447. [CrossRef]
23. Mirakbari, M.; Ebrahimi, K.Z. Evaluation of the climate change effects on the future drought characteristics of Iranian wetlands. *Arab. J. Geosci.* **2021**, *14*, 2167. [CrossRef]
24. Rassoul, Z.A.; Mehdi, M.M.; Bahrami, M. Comparison of reconnaissance drought index (RDI) and effective reconnaissance drought index (eRDI) to evaluate drought severity. *Sustain. Water Resour. Manag.* **2019**, *5*, 1345–1356. [CrossRef]
25. Tsakiris, G. *Meteorological Drought Assessment, Paper Prepared for the Needs of the European Research Program MEDROPLAN*; Mediterranean Drought Preparedness and Mitigation Planning: Zaragoza, Spain, 2004.
26. Tsakiris, G.; Loukas, A.; Pangalou, D.; Vangelis, H.; Tigkas, D.; Rossi, G.; Cancelliere, A. Drought characterization [Part 1. Components of drought planning. 1. 3. Methodological component]. In *Drought Management Guidelines Technical Nnex*; Iglesias, A., Moneo, M., López-Francos, A., Eds.; CIHEAM/EC MED A Water: Zaragoza, Spain, 2007; pp. 85–102.
27. Tigkas, D.; Vangelis, H.; Tsakiris, G. Introducing a modified reconnaissance drought index (RDIe). *Proced. Eng.* **2016**, *162*, 332–339. [CrossRef]
28. Tigkas, D.; Vangelis, H.; Tsakiris, G. An enhanced effective reconnaissance drought index for the characterisation of agricultural drought. *Environ. Process.* **2017**, *4* (Suppl. S1), S137–S148. [CrossRef]
29. Ben, O.D.; Abida, H. Monitoring and mapping of drought in a semi-arid region: Case of the Merguellil watershed, central Tunisia. *Environ. Monit. Assess.* **2022**, *194*, 287. [CrossRef]
30. Syed, F.S.; Adnan, S.; Zamreeq, A.; Ghulam, A. Identification of droughts over Saudi Arabia and global teleconnections. *Nat. Haz.* **2022**. [CrossRef]
31. Donovan, J.; Rutsaert, P.; Domínguez, C.; Peña, M. Capacities of local maize seed enterprises in Mexico: Implications for seed systems development. *Food Sec.* **2022**, *1*, 1–21. [CrossRef]
32. Norzagaray, C.M.; Llanes, C.O.; Gaxiola, A.; González, G.G.E. Meteorological interaction between drought/oceanic indicators and rainfed maize yield in an arid agricultural zone in northwest Mexico. *Arab. J. Geosci.* **2020**, *13*, 131. [CrossRef]
33. Bruno, F.C. La Paradoja de la Economía Sinaloense en la Globalización: Inseguridad Alimentaria en el Granero de México, 1994–2014. Master's Thesis, Universidad Autónoma de Nayarit, Tepique, Mexico, 2016; p. 148.
34. Morales, Z.F. El Impacto de la Biotecnología en la Formación de Redes Institucionales en el Sector Hortofrutícola de Sinaloa, México. Ph.D. Thesis, Universidad de Barcelona, Barcelona, Spain, 2007; p. 441.
35. Llanes, C.O.; Norzagaray, C.M.; Gaxiola, A.; González, G.G.E. Regional precipitation teleconnected with PDO-AMO-ENSO in northern Mexico. *Theor. Appl. Climatol.* **2020**, *140*, 667–681. [CrossRef]
36. Base de Datos del CLICOM. Available online: http://clicom-mex.cicese.mx/mapa.html (accessed on 31 December 2021).
37. Lo Presti, R.; Barca, E.; Passarella, G. A methodology for treating missing data applied to daily rainfall data in the Candelaria River Basin (Italy). *Environ. Monit. Assess.* **2010**, *160*, 1–22. [CrossRef]

38. Johnson, M. Lose Something? Ways to Find Your Missing Data. In Proceedings of the Houston Center for Quality of Care and Utilization Studies Professional Development Series, 17 September 2003. professional development seminar series.
39. Aieb, A.; Madani, K.; Scarpa, M.; Bonaccorso, B.; Lefsih, K. A new approach for processing climate missing databases applied to daily rainfall data in Soummam watershed, Algeria. *Heliyon* **2019**, *5*, e01247. [CrossRef]
40. Ministry of Agriculture, Livestock, Rural Development, Fisheries and Food (SAGARPA) and Agri-Food and Fishing Information Service (SIAP). Available online: http://infosiap.siap.gob.mx/aagricola_siap_gb/ientidad/index.jsp (accessed on 12 December 2021).
41. Hargreaves, G.H.; Samani, Z.A. Estimating potential evapotranspiration. *J. Irrig. Drain. Div.* **1982**, *108*, 225–230. [CrossRef]
42. UNEP (United Nations Environmental Programme). *World Atlas of Desertification*; United Nations: New York, NY, USA, 1992.
43. Ogurinde, A.T.; Emmanuel, I.; Enaboifo, M.A.; Adedayo, A.T.; Bao, P.Q. Spatio-temporal calibration of Hargreaves–Samani model in the Northern Region of Nigeria. *Theor. Appl. Climatol.* **2022**, *147*, 1213–1228. [CrossRef]
44. Bahmani, S.; Salimi, H.; Sanikhani, H. Spatiotemporal analysis of aridity indices by using the nonparametric methods (case study: Sirvan river basin, Kurdistan Province, Iran). *Arab. J. Geosci.* **2021**, *14*, 2034. [CrossRef]
45. Kourgialas, N.N.; Dokou, Z.; Karatzas, G.P. Statistical Analysis and ANN modeling for predicting hydrological extremes under climate change scenarios. The example of a small mediterranean agro-watershed. *J. Environ. Manag.* **2015**, *154*, 86–101. [CrossRef]
46. Proutsos, N.; Tigkas, D. Growth Response of Endemic Black Pine Trees to Meteorological Variations and Drought Episodes in a Mediterranean Region. *Atmosphere* **2020**, *11*, 554. [CrossRef]
47. Potopová, V.; Tűrkott, L.; Musiolková, M.; Možný, M.; Lhotka, O. The compound nature of soil temperature anomalies at various depths in the Czech Republic. *Theor. Appl. Climatol.* **2021**, *146*, 1257–1275. [CrossRef]
48. Aliyar, Q.; Dhungana, S.; Shrestha, S. Spatio-temporal trend mapping of precipitation and its extremes across Afghanistan (1951–2010). *Theor. Appl. Climatol.* **2022**, *147*, 605–626. [CrossRef]
49. Weathington, B.L.; Cunningham, C.J.L.; Pittenger, D.J. *Understanding Business Research: Appendix B: Statistical Tables*; John Wiley & Sons, Inc.: Hoboken, NJ, USA, 2012; pp. 435–483. [CrossRef]
50. Reza, T.I.A.; Alam, N.I.; Hasanuzzaman, M.; Bozlar, R.M.; Elbeltagi, A.; Mallick, J.; Techato, K.; Chandra, P.S.; Mostafizur, R.M. Variability of climate-induced rice yields in northwest Bangladesh using multiple statistical modeling. *Theor. Appl. Climatol.* **2022**, *147*, 1263–1276. [CrossRef]
51. Secretaría de Medio Ambiente y Recursos Naturales (SEMARNAT). *Plan Estatal de Cambio Climático de Sinaloa (PECCSIN)*; SEMARNAT: Mexico City, Mexico, 2016; p. 183.
52. Velasco, I.; Pimentel, E. Zonificación agroclimática de Papadakis aplicada al estado de Sinaloa, México. *Investig. Geográficas. Bol. Inst. Geog.* **2010**, *73*, 86–102.
53. Wei, C.; Guo, B.; Zhang, H.; Han, B.; Li, X.; Zhao, H.; Lu, Y.; Meng, C.; Huang, X.; Zang, W.; et al. Spatial–temporal evolution pattern and prediction analysis of flood disasters in China in recent 500 years. *Earth Sci. Inform.* **2022**, *15*, 265–279. [CrossRef]
54. Nemati, A.; Ghoreishi, N.S.H.; Joodaki, G.; Mousavi, N.S.S. Spatiotemporal Drought Characterization Using Gravity Recovery and Climate Experiment (GRACE) in the Central Plateau Catchment of Iran. *Environ. Process.* **2020**, *7*, 135–157. [CrossRef]
55. Ramírez, B.V.H.; Jaramillo, R.Á. Relación entre el índice oceánico de el niño y la lluvia, en la región andina central de Colombia. *Cenicafé* **2009**, *60*, 161–172.
56. Lavín, M.F.; Palacios, H.E.; Cabrera, C. Sea surface temperature anomalies in the Gulf of California. *Geof. Int.* **2003**, *42*, 363–375.
57. Arriaga, D.A.A. Identificar Patrones de Precipitación en la CDMX en Períodos de Lluvia o Sequía, Asociados con los Índices de los Fenómenos ENSO, AMO, NAO y PDO en los años de 1951 al 2007. Bachelor's Thesis, Instituto Politécnico Nacional, Ciudad de Mexico, Mexico, 2019; p. 150.
58. Llanes, C.O.; Gaxiola, H.A.; Estrella, G.R.D.; Norzagaray, C.M.; Troyo, D.E.; Pérez, G.E.; Ruiz, G.R.; Pellegrini, C.M.J. Variabiity and factors of influence of extreme wet and dry events in northern Mexico. *Atmosphere* **2018**, *9*, 122. [CrossRef]